



Study on controlling the effect of chloride salt erosion and carbonation on the deterioration of shotcrete

Huamou Liu^a, Wanyun Lu^{b*} and Guoming Liu^c

College of Safety and Environmental Engineering; Shandong University of Science and Technology, Taian, China

^a15853705017@163.com, ^{b*}761986638@qq.com
^cskd995978@sdust.edu.cn

Abstract. With the continuous expansion of the marine construction industry in various countries, the number of large-scale marine engineering structures made of concrete, such as bay bridge, port terminals, submarine tunnels etc., is increasing annually. Therefore, it is urgent to study the deterioration mechanism of marine concrete and its disaster prevention and control. In this paper, five types of concrete specimens such as cement paste, cement mortar, and concrete were made and cured under standard curing, carbonation curing, and NaCl erosion conditions for each type of concrete specimens. The results showed that the strengths of cement paste, mortar and concrete were gradually increasing at the same water-cement ratio, which was due to the addition of fine aggregate in mortar densified the pores and cracks of the cement paste and made it more structurally complete, while the addition of coarse aggregate in the concrete assumed a greater mechanical strength. And the microscopic results showed that with the addition of polymer, the structure became dense, and the combination of hydration product C-S-H gel and crystals became closer; when fly ash was added, the encapsulation effect of hydration gel product on unhydrated mineral admixture and crystals was poorer compared with that of ordinary concrete, and microcracks on the cross section also increased significantly, which ultimately led to weaker carbonation resistance.

Keywords: shotcrete, disaster prevention, aggregate type, deterioration mechanism.

1 Introduction

The durability of concrete structures is a major concern all over the world, especially in coastal areas, where the ingress of carbon dioxide and chloride ions can cause corrosion of steel bars. The penetration of carbon dioxide triggers a carbonization reaction in the concrete material. Concrete carbonization is a neutralization phenomenon that involves a reaction between carbon dioxide and hydrated cement compounds, resulting in a decrease in the pH of the concrete pore solution [1-3]. The reduction in the alkalinity of concrete may disrupt the passivation film that initially formed around the rebar, which

© The Author(s) 2024

P. Liu et al. (eds.), *Proceedings of the 2024 5th International Conference on Civil, Architecture and Disaster Prevention and Control (CADPC 2024)*, Atlantis Highlights in Engineering 31,

https://doi.org/10.2991/978-94-6463-435-8_22

can lead to corrosion of the rebar when both moisture and oxygen are present [4-7]. In addition to carbon dioxide intrusion, rebar corrosion can also occur when sufficient amounts of chloride ions accumulate on the surface of rebar [8,9]. Chloride-induced corrosion of rebar reduces the cross-sectional area of rebar, accelerates the formation of cracks in concrete, and even leads to spalling of the concrete protective layer, thereby reducing the remaining service life of concrete structures [10,11]. In some environmental regions, such as the atmosphere and oceanic areas, carbon dioxide and chloride ions can interact, and this coupling effect may lead to the deterioration of materials more quickly than either alone [12].

Based on a review of previous research work, several studies have been conducted to investigate the effects of carbonization on chloride intrusion in cement and concrete materials. For example, Nasser et al. [13] reported that higher ratios of water-soluble chloride to acid-soluble chloride content can be formed in the presence of carbonation. Dong et al. [14] noted that carbonization leads to the release of bound chlorides in concrete materials and a sudden increase in the concentration of free chlorides. In addition, the chloride diffusion rate in concrete materials can be significantly increased by carbonization, as demonstrated by Xian et al. [15], Bahman-Zadeh et al. [16], and Da et al. [17-18] in their article. This finding is also supported by an experimental study that used X-ray computed tomography [19] to study the effect of chloride ions on the carbonization of cement slurries. The researchers found that increasing the chloride ions in the cement slurry could refine the porous structure and reduce the porosity. As a result, the resistance of the cement slurry to CO₂ permeability is improved. Dias et al. [20-21] pointed out that when concrete structures are subjected to the dual environmental effects of carbonization and chloride intrusion, the risk of reinforcement corrosion due to carbonization (assuming the presence of both moisture and oxygen) is less severe than that caused by chloride erosion.

The innovation of this research is to study the type of aggregate of normal silicate concrete on its deterioration mechanism study as well as the mixing of fly ash and polymers on its resistance to deterioration. The concrete damage mechanism was analyzed by carbonation curing and chloride salt erosion conditions on concrete specimens. The mechanical properties and carbonation depth of the specimens after curing were tested, and the microscopic properties of concrete under various erosion conditions were investigated using scanning electron microscope (SEM) and X-ray diffractometer (XRD) techniques.

2 Experimental work

2.1 Materials and specimen preparation

In this experiment, Shanshui brand P·O 42.5 type cement, with a specific surface area of 344 m²/kg, a preliminary setting time of 206 minutes and a final setting time of 269 minutes, conforms to GB175-2007 standard. Instead of cement, first-class fly ash is selected, and the main chemical composition is shown in Table 1. River sand with a fineness modulus of 2.2-3 is used for fine aggregates, and gravel with a particle size of 5-15 is used for coarse aggregates, and the distribution curve is shown in Figure 1.

NaCl is made of analytical pure sodium chloride produced by Sinopharm Chemical Reagent Co., Ltd., and its content is greater than or equal to 99.5%. The carbonization depth indicator is phenolphthalein indicator produced by Yida Technology Co., Ltd., with a concentration of 1% and a color development range: pH 8.2-10. The polymer is a polyacrylate emulsion produced by Beijing Mengtai Weiye Building Materials Co., Ltd., and the analysis net is greater than or equal to 90%.

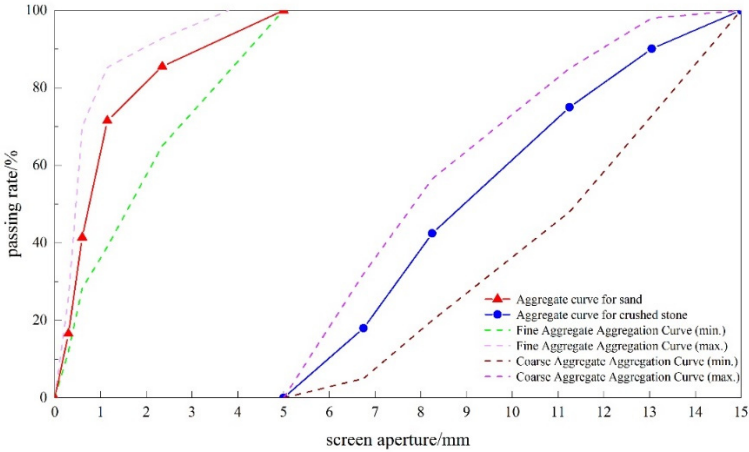


Fig. 1. Aggregate Aggregate Curve

Table 1. Main chemical composition of cement and fly ash

Main chemical composition	SiO ₂	Al ₂ O ₃	Fe ₂ O ₃	CaO	MgO	K ₂ O	Na ₂ O	TiO ₂	SO ₃	Cl ⁻
Cement	15.03	3.99	4.53	62.37	4.35	1.11	0.19	0.37	1.82	0.04
Fly ash	42.83	23.03	2.55	5.62	0.95	1.37	0.41	1.72	0.76	0.02

In this paper, we will explore the erosion mechanism of chloride ions on concrete aggregates, so different aggregate compositions are designed to observe the performance changes of concrete under the same curing conditions and different curing conditions. At the same time, based on the background of carbon peak and carbon neutrality, this paper designs carbonization curing conditions, discusses the content of carbon dioxide absorbed in the process of concrete compaction, observes its performance changes, contrasts with standard curing conditions, observes the changes in the properties of concrete after carbon dioxide absorption during the compaction process, and analyzes the deterioration mechanism.

The concrete cube specimens with design sizes of 100 mm × 100 mm × 100 mm were placed in the mold after pouring, and then demolded after 24 hours of molding, and three different curing conditions were designed, as shown in Table 2, and cured for 28 days under each condition.

Table 2. Specimen mixing ratio for each group(components kg/m³)

Experimental group	Water	Cemet	Sand	coarse aggregate	polymers	Fly ash	Water reducing agent
Cement paste	600	1200	-	-	-	-	-
Mortar	227.55	455.1	1023.82	-	-	-	-
Concrete	208.425	416.85	937.913	625.28	-	-	0.8337
Concrete with polymer	208.425	416.85	937.913	625.28	41.69	-	0.8337
Concrete with fly ash	208.425	235.67	937.913	625.28	-	177.3	0.8337

Table 3. Experimental conservation conditions

Experimental group	Conservation model
S	Standard maintenance
N	NaCl erosion conditions
C	Carbonization box maintenance

In this paper, a total of 15 sets of tests will be carried out, consisting of five types of specimens as shown in Table 2 and three curing conditions in Table 3. In Table 3, the control humidity is 70%±5%, the temperature is 20°C±3°C, and the carbon dioxide concentration is 20%±3 in the CCB-70F-20% concrete carbonization test chamber. Shi Caijun et al. analyzed the feasibility of carbon dioxide conservation, which also met the requirements of carbonization test. The left picture of Figure 2 is the CCB-70F-20% concrete carbonization test chamber, and the right is the standard curing conditions of the concrete: the temperature is 20±2 °C within 28 days, and the humidity will not be less than 95%.

**Fig. 2.** Conservation conditions (carbonization conservation on the left; standard conservation on the right)

2.2 Test Method

Mechanical property test.

According to the five kinds of test blocks shown in Table 2, the standard iron triple is selected to prepare and cure the concrete test blocks under the regulations, and each group of experiments prepares 30 test blocks of the same batch of mixing and pouring, a total of 90 pieces, and the curing time is 28 days. After the concrete specimen is cured for 28 days, the concrete compressive and concrete splitting resistance tests are carried out. The tests were performed on a SHIMADZU AGX-250 pressure testing machine, as shown in Figure 3. In order to reduce the test error, each group of experiments was tested with three concrete specimens made in the same batch, and the average value was taken. It is carried out in strict accordance with GB/T 50081-2002 "Standard for Test Methods for Mechanical Properties of Ordinary Concrete".



Fig. 3. Digital display pressure tester

2.3 Ultrasonic defect analysis

The ultrasonic defect detection and analysis of concrete was carried out using the HC-U83 non-metallic ultrasonic detector, as shown in Figure 4. The instrument emits 20-500 Hz sound waves, and has two interfaces divided into transmitter and receiver, and the sound wave enters the concrete through the transmitter end. However, when there are more pores and cracks inside the concrete, and there is an air medium inside the concrete, when the sound wave is transmitted inside the concrete, the sound speed will change because of the different mediums, and the amplitude and frequency of the sound wave will also change accordingly. However, the loss of sound velocity in concrete is small, and the development degree of internal cracks in various types of concrete cannot be obviously compared, so the amplitude of sound waves is used as a

measurement standard, and the standard deviation of the amplitude is analyzed to characterize the development of internal cracks in concrete.

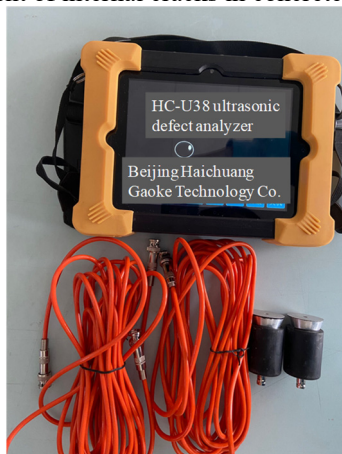


Fig. 4. HC-U38 Ultrasonic defect analyzer

Carbonization depth test

The carbonization depth test will use the experimental method shown in Figure 5 to determine the carbonization depth, the concrete will be placed in the carbonization test chamber for curing, after curing for 28 days, the 100 mm×100 mm×100 mm test block will be cut from it, the alcohol-phenolphthalein solution (Phenolphthalein-alcohol indicator has a color range of pH 8.2-10) with a concentration of 1% will be titrated to the concrete section, and finally the uncolored part will be measured with vernier calipers.



Fig. 5. Carbonization depth test test

XRD analysis

The specimens in the standard maintenance and the specimens after a certain corrosion cycle were milled or drilled for sampling, and placed in an oven at 40°C for drying for 12 h. The milled and drilled samples were passed through a square hole sieve of 0.075 mm, and the sieve residue was taken for testing. D8 ADVANCE X-ray diffractometer was used for the test. The target material used in the experiment was Cu target, 2θ was 10~90°, and the scanning speed was 4°/min.

SEM scanning electron microscope analysis

Hand-held cutting machine to be tested sample from the cementitious materials from the internal removal, selection of sample size of about 1cm³, after the specimen by the resin curing, grinding, polishing and other processes, and then sprayed platinum treatment, and then QUANTA FEG 450 field emission scanning electron microscope to observe, and with the corresponding spectrometer on the observed microstructure for Compositional analysis.

TG-DTG analysis

The above milling samples were subjected to thermogravimetric analysis, and the changes in the relative content of corrosion products were analyzed using a comprehensive thermal analyzer model STA449F3 produced by NETZSCH GmbH, Germany. The test gas was air, the selected heating rate was 10°C/min, and the temperature range of the test was from 30°C to 800°C.

3 Results and Discussion

3.1 Analysis of Macro Physical Properties

As can be seen in Fig. 6, the compressive strength values of all types of specimens after 28 days of standard curing are maximum, which demonstrate that concrete hydration must occur under sufficiently moist conditions. The amount of harmful ions to concrete in the experimental water is low. After 28 days of standard maintenance, it can reach 1.1 times to 1.3 times in NaCl erosion condition. This is 10-50% higher than under carbonized conditions. Under standard indoor curing conditions, the hydration reaction of concrete is more complete and thorough, and there are a large number of relatively dense hydrated silicates at the section, which can fill the gaps between aggregates while coagulating the aggregates well. This is due to the early stage of concrete curing due to the existence of more internal pores, carbon dioxide into the interior of the concrete matrix, carbon dioxide gas dissolved in water will be generated with the concrete Ca(OH)₂ calcium carbonate, although effective in enhancing the strength of concrete curing at the beginning of the curing process. But with the growth of the age of curing, the increase in calcium carbonate leads to the expansion of the concrete internal deformation, and ultimately reduce the 28-day compressive strength. Similarly, the water content is higher when the specimen is completely immersed in 5% NaCl solution, but the 5% NaCl solution will affect the hydration process of the concrete and the harmful

ions enter into the interior of the concrete through the pores and cracks, reducing the compressive strength of the specimen.

Figure 7 demonstrates the splitting strength of various specimens at 28 days. Compared with the concrete mixed with fly ash, the compressive strength of standard concrete and concrete mixed with polymers is higher, the reason is that due to the addition of fly ash, making the specimen internal pore increase, in the early stage of curing so that the internal pore is in a negative state, the harmful ions in the solution into the micropores to form a crystalline filler, as well as the chemical reaction, the generation of Aft, Gyp or Friedel The generation of Aft, Gyp or Friedel's salt makes the pores dense, and the generation of F salt will preferentially combine with concrete $\text{Ca}(\text{OH})_2$, leading to the reduction of the rate of generation of stabilized C-S-H, which ultimately leads to the reduction of compressive strength of concrete. Porosity reduction, although the initial compressive strength increased, but with the growth of the maintenance time, the compressive strength gradually decreased, is due to the tensile strength of the concrete matrix will be less than the internal expansion stress and osmotic compressive stress and other internal stresses, resulting in the concrete surface mortar fall off, the quality of the final result of the decline in compressive strength.

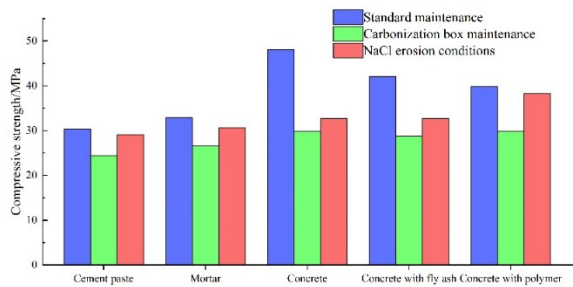


Fig. 6. Compressive strength of different specimens

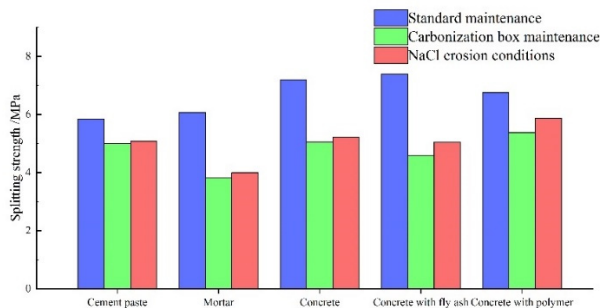


Fig. 7. Splitting strength of different specimens

3.2 Carbonization depth test

Where the figure 8 depicts three points for each type of specimen representing the depth of carbonation of concrete for 28 days under standard curing, carbonation box curing, and NaCl erosion conditions, where the carbonation box curing condition has the highest depth of carbonation, and the standard curing and NaCl erosion conditions do not have a significant effect on the depth of carbonation of concrete. The carbonation depth of carbonation box curing was 1.1 times to 1.3 times higher than that of standard curing, which indicates that carbonation curing accelerates the carbonation process of concrete. Excessive admixture of mineral admixture will lead to low initial pH of concrete pore solution, with the invasion of CO_2 , $\text{Ca}(\text{OH})_2$ content is decreasing, the resistance to CO_2 diffusion is weakened, resulting in damage to the carbonation resistance, and the densification effect of fly ash and slag on the pore space can not compensate for this part of the damage.

At the same time, when the amount of admixture is too large, the mineral admixture secondary hydration can not react adequately, and the unhydrated particles piled up between the paste and aggregate, which will reduce the compactness of concrete, increase the diffusion channel of CO_2 , and make the anti-carbonation performance obviously deteriorate. At the same time, the reaction product of fly ash can compact the internal structure of concrete, but at the same time, SiO_2 and Al_2O_3 in fly ash will consume the alkaline material in the concrete void liquid, making the concrete resistance to CO_2 erosion weakened, and finally make the concrete carbonation deepen.

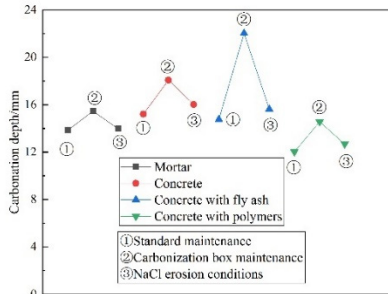


Fig. 8. Carbonization depth of various specimens

3.3 Ultrasonic defect analysis

According to table 4, we can learn that carbonation curing is the curing condition with the largest standard deviation under the three curing conditions, and the standard deviation of all kinds of specimens under carbonation curing condition is 1.6~2.4 times of that under standard curing condition, among which the amplitude of mortar ultrasonically detected in carbonation box is 2.4 times of that under standard curing condition. Figure 9 illustrates the acoustic wave amplitude curves for various conservation con-

ditions. Through the standard deviation of various types of specimens, we can see that the standard deviation of the amplitude of fly ash-doped concrete is the largest, indicating that it has the most internal pores and cracks, and its strength is lower than that of concrete and polymer-doped concrete when compressive strength and rupture strength are tested. It can be learned that the more obvious the internal cracks of each type of specimen, the lower its compressive strength and rupture strength, and they show a linear correlation. When compared with the previous carbonation depth test, the amplitude change of concrete under carbonation condition is most obvious which is consistent with the previous carbonation depth test results, and the carbonation depth of standard curing and NaCl erosion are lower than that of concrete under carbonation condition.

Table 4. Ultrasonic testing sound wave amplitude table for various specimens

	Mortar	Concrete	Concrete with fly ash	Concrete with polymers
Standard maintenance	1.417618	1.14252	2.593857	0.685583
Carbonization maintenance	3.430504	1.625152	4.817195	1.146762
NaCl erosion conditions	1.352559	1.150207	2.244826	0.716185

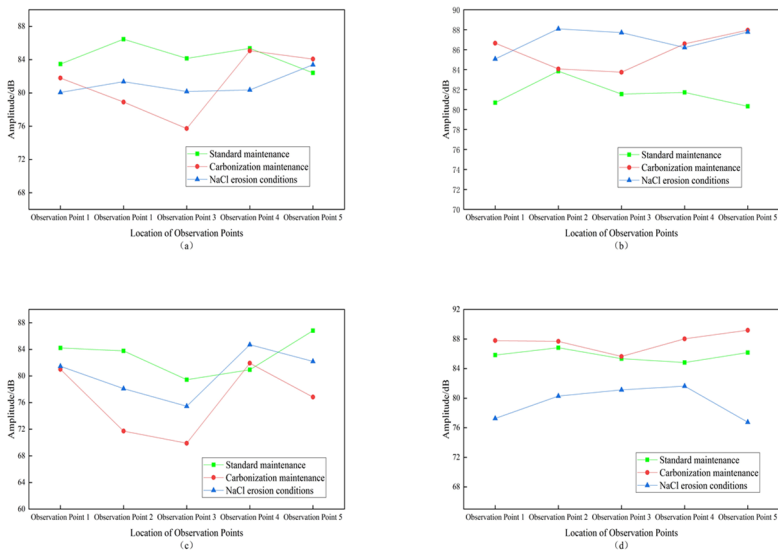


Fig. 9. Ultrasonic wave amplitude of various specimens (a) mortar wave amplitude; (b) concrete wave amplitude; (c) fly ash mixed concrete wave amplitude; (d) polymer mixed concrete wave amplitude

3.4 SEM scanning electron microscopy analysis

Figures 10 to 12 show SEM images of concrete under various curing conditions and images observed under a Leica microscope, and it is found that with the addition of polymer, the structure becomes dense, and the combination of hydration product C-S-H gel and crystals becomes more compact; when the mineral admixture dosage is added, the encapsulation effect of hydration gel product on the unhydrated mineral admixture and crystals is poorer compared with that of ordinary concrete, and the micro-cracks on the cross-section are also obviously increased.

Comparison of group images can be obtained from the effect of single-mixed fly ash admixture on the microscopic morphology, the number of C-S-H gel and $\text{Ca}(\text{OH})_2$ crystals inside the concrete decreases with the increase of fly ash admixture, fly ash admixture of 20% of group B net mortar specimens microscopic structure performance is more dense, and the degree of denseness of pure cement concrete is not much different, analyze the reason for this is that: fly ash admixture of 20%, the second fly ash The reason is that at 20% fly ash dosage, the secondary reaction of fly ash can be fully carried out, and the secondary hydration products also have the effect of filling the internal voids, so the microstructure is more dense, and the presence of complete $\text{Ca}(\text{OH})_2$ crystals can be easily observed in both groups A and B of the net mortar specimens.

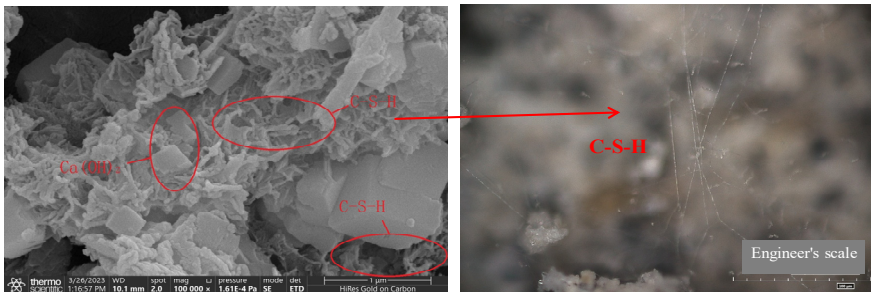


Fig. 10. Standard maintenance 28 days picture, the left picture is SEM scanning electron microscope picture, the right picture is the picture under Leica microscope

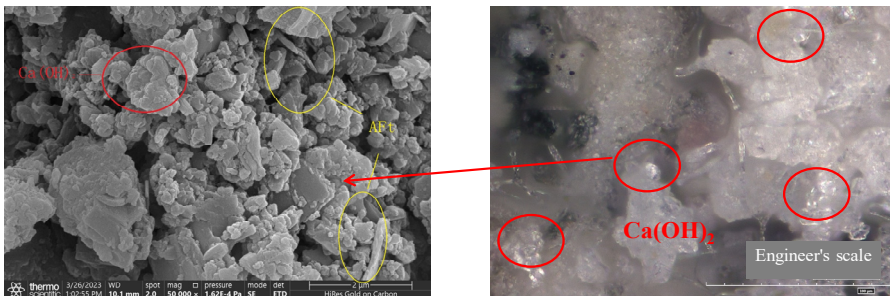


Fig. 11. Carbonization maintenance 28 days pictures, the left picture is SEM scanning electron microscope picture, the right picture is under the Leica microscope picture

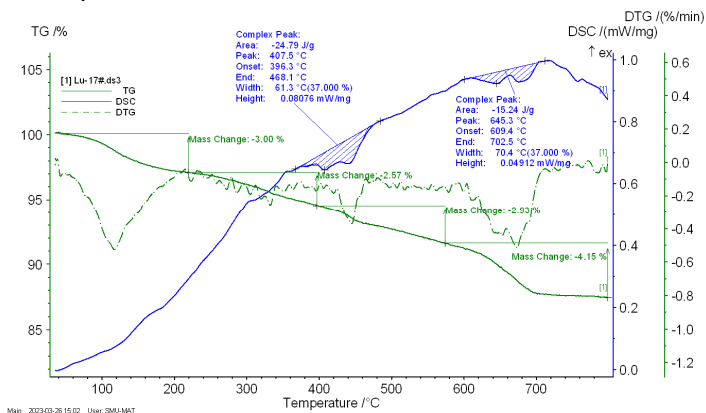


Fig. 12. Pictures of NaCl erosion conditioned for 28 days, SEM scanning electron microscope pictures on the left, and pictures under Leica microscope on the right

3.5 TG-DTG analysis

The damage destruction of cementitious materials by chloride ion and carbonation conditions involves a series of physicochemical changes, in order to study the damage deterioration mechanism and law of cementitious materials under different corrosive media. TG-DTG comprehensive thermal analysis was used to quantitatively analyze the concrete samples exposed to chloride ion and carbonation conditions.

The damage destruction of cementitious materials by chloride ion and carbonation conditions involves a series of physicochemical changes. In order to study the damage deterioration mechanism and law of cementitious materials under different corrosive media, the net paste samples exposed to chloride ion and carbonation conditions were quantitatively analyzed by using TG-DSC integrated thermal analysis. As can be seen from Fig. 13, the specimens before corrosion had three distinct weight loss stages, while all the net mortars appeared to have one distinct weight loss stage after different maintenance conditions. Among them, 80~150°C mainly involves C-S-H gel dehydration, free water dissipation and calomel dehydration stages, 420~480°C mainly involves $\text{Ca}(\text{OH})_2$ decomposition resulting in weight loss, and 680~800°C corresponds to thermal decomposition of CaCO_3 .



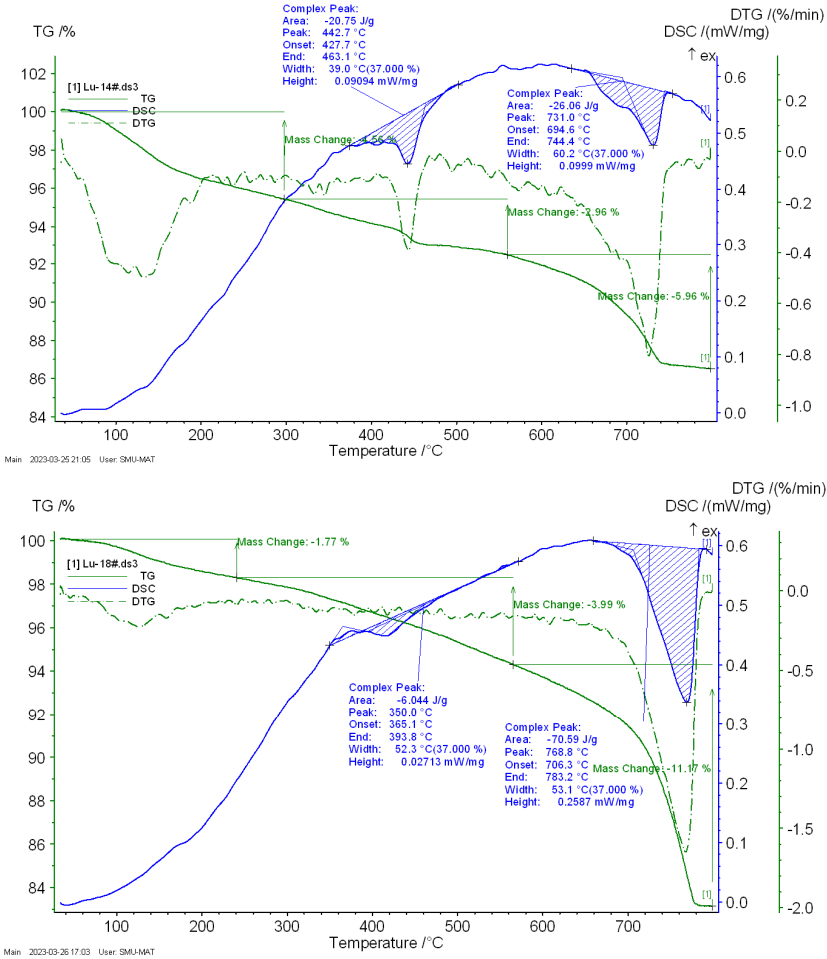


Fig. 13. From left to right, the TG-DTG curves for standard concrete curing, NaCl erosion conditions, carbonation curing

3.6 XRD analysis of hydration products

Figure 14 shows the standard curing conditions in the plots can be observed, the five groups of specimens in the hydration products are basically the same, but with the incorporation of fly ash, the content of the carbonatable material $\text{Ca}(\text{OH})_2$ in the concrete is reduced, which leads to a deterioration in the carbonation resistance of the concrete, the incorporation of polymers did not change the components significantly. The SiO_2 phase in the polymer-infused concrete was the highest among all types of specimens, indicating that its hydration process was the slowest; while the C-S-H phase of the concrete was the highest, and at the same time its mechanical properties were the best, indicating that the mechanical properties of concrete are determined by its C-S-H.

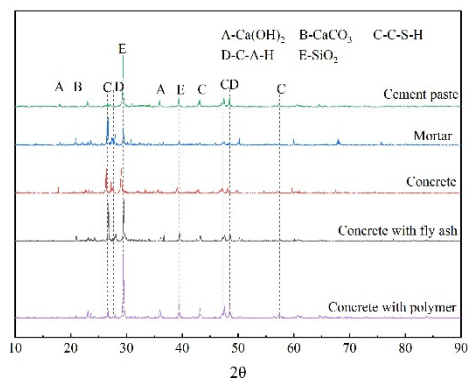


Fig. 14. XRD images of hydration products under standard curing conditions of various specimens

4 Conclusions

In this paper, a total of 15 sets of experiments were designed using the crossover design method to systematically investigate the evolution patterns of mechanical properties and carbonation resistance at different ages under four influencing factors, namely, concrete aggregate type (cement paste, mortar, and concrete), concrete with single admixture of fly ash, concrete with admixture of polymers, and curing conditions (standard curing, carbonation curing, and NaCl erosion conditions), and the degree of correlation between them and the carbonation resistance. The degree of correlation between them and the carbonation resistance. Combined with the microscopic test results of scanning electron microscope (SEM) microscopic images, ultrasonic detection analysis, X-ray diffraction pattern (XRD) and thermogravimetric analysis method (TG-DTG), the influencing mechanism of the carbonation resistance performance is analyzed. There are several conclusions in this paper as follows:

(1) The changes in mechanical properties and microstructure of fly ash-added and polymer-added concrete under chloride salt and carbonation conditions were investigated by comparing with OPC. The results show that the strength of cement paste, mortar, and concrete at the same water-cement ratio is gradually increasing, which is due to the addition of fine aggregate in mortar densifies the pore cleavage of the cement paste and makes it more structurally intact; while the addition of coarse aggregate in the concrete bears greater mechanical strength; However, the mechanical strength of shotcrete degrades over time, so further research is needed to examine the underlying mechanisms of these trends and to develop new techniques or materials to minimize the loss of strength over time and improve long-term performance.

(2) When the specimen blocks were cured in the carbonation box and when they were completely immersed in 5% NaCl solution, both of them affected the hydration process of the concrete and changed its micro-morphology, as well as had an effect on

its mechanical properties; However, the aspect of its permeability of shotcrete has not been adequately studied in this paper, in addition, the relationship between the interactions between the microstructure of shotcrete by admixtures such as quicklime and air-entraining agents and the resistance to carbonation, sulphate and chloride erosion needs to be further investigated in order to understand their combined effect on the permeability of shotcrete.

(3) By observing the microscopic morphology of each group of hardened specimens, it was found that with the addition of polymer, the structure became dense, and the combination of hydration product C-S-H gel and crystals became more tight; when adding mineral admixture admixture, the encapsulation effect of the hydration gel product on the unhydrated mineral admixture and crystals was worse compared with that of ordinary concrete, and the microcracks on the cross-section also increased significantly.

Acknowledgement

This study was funded by projects such as National Natural Science Foundation of China (Grant No. 52274219); Shandong Provincial Youth Innovation Team Development Plan (No. 2022KJ213); Qingdao West Coast New Area Source Innovation Project (2021-111); Special funds for Taishan scholar project.

References

1. Dong B, Qiu Q., Xiang J, et al. (2014) Electrochemical impedance measurement and modeling analysis of the carbonation behavior for cementitious materials, *Constr. Build. Mater.* 54: 558–565. <https://doi.org/10.1016/j.conbuildmat.2013.12.100>.
2. Marques P.F., Chastre C., Nunes Â. (2013) Carbonation service life modelling of RC structures for concrete with Portland and blended cements, *Cement. Concrete. Compos.* 37: 171–184. <https://doi.org/10.1016/j.cemconcomp.2012.10.007>.
3. **, M., Dangla, P. & Li, K. (2021) Reactive transport modelling of concurrent chloride ingress and carbonation in concrete. *Mater Struct* 54: 177-191. <https://doi.org/10.1617/s11527-021-01769-9>.
4. AL-Ameeri A S, Rafiq M I, Tsioulou O. (2021) Combined impact of carbonation and crack width on the Chloride Penetration and Corrosion Resistance of Concrete Structures. *Cement and Concrete Composites*, 115:103-819. <https://doi.org/10.1016/j.cemconcomp.2020.103819>.
5. Zheng Y, Russell M, Davis G, et al. (2021) Influence of carbonation on the bound chloride concentration in different cementitious systems. *Construction and Building Materials*, 302: 124-171. <https://doi.org/10.1016/j.conbuildmat.2021.124171>.
6. Dang V Q, Ogawa Y, Bui P T, et al. (2021) Effects of chloride ions on the durability and mechanical properties of sea sand concrete incorporating supplementary cementitious materials under an accelerated carbonation condition. *Construction and Building Materials*, 274: 122-016. <https://doi.org/10.1016/j.conbuildmat.2020.122016>.
7. Malheiro R, Camões A, Meira G, et al. (2020) Effect of coupled deterioration by chloride and carbonation on chloride ions transport in concrete. *RILEM Technical Letters*, 5: 56-62. <https://doi.org/10.21809/rilemtechlett.2020.126>.

8. Liu W, Li Y.Q., Tang L.P., Xing F. (2021) Modelling analysis of chloride redistribution in sea-sand concrete exposed to atmospheric environment. *Construction and Building Materials*, 274: 121-962, 0950-0618, <https://doi.org/10.1016/j.conbuildmat.2020.121962>.
9. Dong B., Qiu Q., Gu Z., et al., (2016) Characterization of carbonation behavior of fly ash blended cement materials by the electrochemical impedance spectroscopy method. *Cem. Concr. Compos*, 65:118–127. <https://doi.org/10.1016/j.cemconcomp.2015.10.006>.
10. Dousti A, Khaksar H. (2023) Impact of Simultaneous Carbonation and Chloride Attack on Chloride Diffusion in Portland Cement Concrete Mixtures Blended with Natural Zeolite and Silica Fume. *Journal of Materials in Civil Engineering*, 35(12): 0402-3478. <https://doi.org/10.1061/JMCEE7.MTENG-15253>.
11. Li D W, Li L, Li P, Wang Y. (2022) Modelling of convection, diffusion and binding of chlorides in concrete during wetting-drying cycles, *Marine Structures*, 84: 0951-8339, <https://doi.org/10.1016/j.marstruc.2022.103240>.
12. Mallek J, Daoud A, Omikrine-Metalssi O, Loulizi A. (2021) Performance of self-compacting rubberized concrete against carbonation and chloride penetration. *Structural Concrete*; 22: 2720–2735. <https://doi.org/10.1002/suco.202000687>.
13. Nasser A., Clément A., Laurens S., Castel A., (2010) Influence of steel–concrete interface condition on galvanic corrosion currents in carbonated concrete. *Corros. Sci.* 52: 2878–2890. <https://doi.org/10.1016/j.corsci.2010.04.037>.
14. Dong B., Qiu Q., Xiang J., et al., (2014) Study on the carbonation behavior of cement mortar by electrochemical impedance spectroscopy. *Materials* 7: 218–231. <https://doi.org/10.3390/ma7010218>.
15. Xian X.P., Zhang D., Shao Y., Zhang S.P. (2023) Evaluation of corrosion resistance of precast reinforced concrete subjected to early-age ambient pressure carbonation curing by accelerated impressed current method. *Journal of Sustainable Cement-Based Materials*, 12:5, 592-608, <https://doi.org/10.1080/21650373.2022.2098200>.
16. Bahman-Zadeh F, Ramezani-pour A A, Zolfagharnasab A. (2022) Effect of carbonation on chloride binding capacity of limestone calcined clay cement (LC3) and binary pastes. *Journal of Building Engineering*, 52: 104447. <https://doi.org/10.1016/j.jobe.2022.104447>
17. Da, B., Li, Y., Yu, H. *et al.* (2022) Effect of Carbonation and Drying-Wetting Cycles on Chloride Diffusion Behavior of Coral Aggregate Seawater Concrete. *J. Ocean Univ. China* 21: 113–123. <https://doi.org/10.1007/s11802-022-4847-z>.
18. Da, B., Yu, H. F., Ma, H. Y., and Wu, Z. Y., (2020) Reinforcement corrosion research based on electrochemical impedance spectroscopy for coral aggregate seawater concrete in a sea-water immersion environment. *Journal of Testing and Evaluation*, 48: 1537–1553, <https://doi.org/10.1520/JTE20180197>.
19. Ye H., Jin X., Fu C., Jin N., Xu Y., Huang T., (2016) Chloride penetration in concrete exposed to cyclic drying-wetting and carbonation, *Constr. Build. Mater.* 112: 457–463. <https://doi.org/10.1016/j.conbuildmat.2016.02.194>.
20. Dias R L, Beltrame N A M, Gonzalez J R, et al. (2023) Effect of duration and pressure of carbonation curing on the chloride profile in concrete. *Revista IBRACON de Estruturas e Materiais*, 16: e16603. <https://doi.org/10.1590/s1983-41952023000600003>.
21. Etxeberria M, Castillo S. (2023) How the Carbonation Treatment of Different Types of Recycled Aggregates Affects the Properties of Concrete. *Sustainability*, 15(4): 31-69. <https://doi.org/10.3390/su15043169>.

Open Access This chapter is licensed under the terms of the Creative Commons Attribution-NonCommercial 4.0 International License (<http://creativecommons.org/licenses/by-nc/4.0/>), which permits any noncommercial use, sharing, adaptation, distribution and reproduction in any medium or format, as long as you give appropriate credit to the original author(s) and the source, provide a link to the Creative Commons license and indicate if changes were made.

The images or other third party material in this chapter are included in the chapter's Creative Commons license, unless indicated otherwise in a credit line to the material. If material is not included in the chapter's Creative Commons license and your intended use is not permitted by statutory regulation or exceeds the permitted use, you will need to obtain permission directly from the copyright holder.

